RSC Advances

ROYAL SOCIETY OF CHEMISTRY

www.rsc.org/advances

The adsorption and photocatalysis behavior of zinc tetra (4-carboxyphenyl) porphyrin sensitized titanate nanotubes

Huigang Wang,[*a,b] Ying Fu,[a] Tiehu Han,[a] Junmin Wan[a] and Xuming Zheng[*a]

Received (in XXX, XXX) Xth XXXXXXXXX 20XX
DOI:

[a]*Department of Chemistry and Engineering Research Center for Eco-dyeing and Finishing of Textiles, MOE, Zhejiang Sci-Tech University, Hangzhou 310018, China*
[b]*Department of Physics, University of Osnabrueck, 49069 Osnabrueck, Germany*

CORRESPONDING AUTHOR FOOTNOTE

Professor Ph.D. Huigang Wang

Email: zdwhg@163.com, huigwang@uni-osnabrueck.de

Department of Chemistry Phone: 00186-571-8684-3627

Zhejiang Sci-Tech University FAX: 00186-571-8684-3627

Hangzhou, 310018

China

Professor Xuming Zheng Email: zhengxuming126@126.com

State Key Laboratory of ATMMT(MOE), Phone: 86-571-86843699

Zhejiang Sci-Tech University FAX: 86-571-86843702

Hangzhou, 310018

China

Abstract:
zinc tetra(4-carboxyphenyl) porphyrin sensitized titanate nanotubes，denoted as ZnTCPP-TNTS，were synthesized with hydrothermal treatment of ZnTCPP-TiO_2 gel and their properties of photo-generated reactive species, holes and electrons were studied by transient absorption spectroscopies. The recombination of holes and electrons in ZnTCPP-TNTS was found to be on the order of picoseconds due to ultra fast free electrons. The time-correlated single-photon counting (TCSPC) technique combined with confocal fluorescence microscopy revealed that the fluorescence intensity of ZnTCPP is weakened dramatically and with lifetime shortened by TNTS under UV excitation. The specific surface areas of prepared ZnTCPP-TNTS reach 335.3 m^2/g determined by N_2 adsorption/desorption and decreased with the increase of calcine temperature. The products were characterized with TEM, SEM and XRD. Adsorption and photocatalysis of methylene blue (MB) over ZnTCPP-TNTS were systematically investigated. The sorption kinetic of MB can be described by the pseudo-second-order model, and the thermodynamics fitted well with monolayer Langmuir adsorption isotherm model. These high surface areas with the twofold removal properties and easier separation ability for recycling use show promising prospect for the treatment of dye pollutants from wastewaters in future industrial application.

Keywords: ZnTCPP-TNTS, Hydrothermal treatment, recombination of holes and electrons, Adsorption and photocatalyst, recycling use

1 Introduction

Anatase-typed TiO_2 is the most commonly utilized photocatalyst because of its efficient photo-activity,high stability, low cost and environment friendly properties[1-6]. However, anatase is a large band-gap semiconductor with absorption wavelength mostly located short than 385 nm[7]. To make better use of the natural solar energy, the development of lower band-gap visible light activated photocatalysts is strongly urged[7-9]. Among the works on the extension of photoresponse to visible light, dye sensitization is regard as an effective strategy in view of low cost and feasibility[10-12]. metalloPorphyrins, such as zinc, tin and copper porphyrins, are excellent photosensitizers because of their long triplet state lifetime, the small singlet-triplet splitting and the high quantum yield for intersystem crossing[13-15]. The sensitized TiO_2 systems can present an enhanced photoactivity compared with the corresponding bare TiO_2 samples under natural solar light irradiation[14, 15], and in particular, the metalloporphyrin complex was shown to be the best one[14]. In this paper, zinc tetra(4-carboxyphenyl) porphyrin were synthesized and were sensitized on titanate nanotubes.

photodegradation of organic pollutants in aqueous media is a timely topic especially in view of the environmentally sustainable development and thus attracts the attention of both academic and industrial research[9, 16]. In the recent years the use of titanate nanotubes as adsorbents and photocatalysts for wastewater treatment has attracted remarkable interest due to their large specific surface areas, high pore volumes, and high density of functional hydroxyl group[17-21]. Photocatalytic degradation is a surface science which process on the interface of the catalysts and the pollutants in aqueous solutions[22-25]. Generally, the preliminary adsorption of organics on the catalyst surface is a prerequisite for highly efficient photodegradation[22-24]. In the removal of dyes titanate nanotubes act as the twofold roles of adsorbent and photocatalyst in the same

time[26], and the adsorption process plays a significant positive role in the catalytic reaction[22-24]. However the heavy density absorption might have an adverse effect on the degradation process[27].

A better understanding of the mechanism for the photo-catalytic reactions of dye sensitized TiO_2 is extremely important for improving the degradation efficiency and rate for practical applications[25]. We all known that photocatalytic degradation rate depends on the interaction between photocatalyst and pollutant and good adsorption capacity can improve the efficiency of photocatalytic degradation[22-24]. So it is important to investigate the adsorption process of organtic pollutants on the surface of titanate to explain the mechanism of photocatalytic reactions[20, 21]. In this paper, ZnTCPP-TNTS were prepared by a hydrothermal reaction, whereafter the as-prepared nanotubes were calcined at a constant temperature. The effects of the calcined temperature on the crystalline structures, specific surface area and whereafter the catalysis performance were investigated. The recombination properties of photo-generated holes and electrons were studied by transient absorption spectroscopies and confocal fluorescence microscopy. Besides, we obtain the kinetic and equilibrium equation from the experimental data to clarify the photocatalytic degradation mechanism of ZnTCPP-TNTS.

2. Experimental Methods

2.1 Apparatus

UV-Vis Cary 50 (Shimadzu corporation,Japan) was used to measure the concentration of MB. The ZnTCPP-TNTS X-ray diffraction (XRD) patterns were recorded on D5000 Diffraction system. The morphology of ZnTCPP-TNTS was determined by Scanning Electron Microscopy (SEM).The Brunauer-Emmett-Teller (BET) surface area was determined in the relative pressure (P/P_0) range of 0.05~0.35.

2.2 Reagents

MB (purity ≥98.5%,Tianjin Chemical Reagents Company,Tianjin,China) and propanoic acid (Tianjin Kemiou Chemical Reagent Company,Tianjin,China) were used as received. Parahydroxybenzaldehyde、tetrabutyl titanate and pyrrole were purchased as analytical reagent for further treatment. Other chemicals such as ethanol and DMF were purchased as analytical reagent. All the solutions used in the experiment were prepared with deionized water.

2.3 ZnTCPP-TNTS preparation[28]

2.3.1 The synthesis of ZnTCPP

First, in the round bottomed flask,6.0g Parahydroxybenzaldehyde was added into 130mL propanoic acid solution,then droping into the 2.8 mL distilled pyrrole slowly at 140□.After stirring for 12 h, the product was filtered ,then recrystallization with the solvent of THF. Finally, we obtained the product of TCPP (tetra(4-carboxyphenyl) porphyrin).

ZnTCPP was prepared by mixing 0.5g TCPP with 1.2g $Zn(AC)_2$ in the solvent of CH_2Cl_2 and DMF (V_{CH2Cl2}:V_{DMF}=1:1) ,after heating reflux for 2 h, cooling it to room temperature , and then adding in 120 mL deionized water, staying overnight , then washing and vacuum drying to obtain ZnTCPP .

2.3.2 The synthesis of ZnTCPP-TiO_2 gel

Firstly, 60mg ZnTCPP was added into 16 mL anhydrous alcohol ,then we get the purple solution which was named as solution A, secondly dropping into 4mL tetrabutyl titanate in A, following adding some chemical addition agents in sequence: 0.6 mL acetylacetone、0.4 mL DMF

and 0.2 mL pyridine under drastic stir for 30 min. Thirdly we add the mixed solution of 2mL deionized water and 4mL anhydrous alcohol into A and controlling the pH 3-4 with hydrochloric acid simultaneously. Secondly, the sample was stired for 2h, then aging under room temperature. Next, calcining to 100 □, so we got the gel.

2.3.3 ZnTCPP-TNTS synthesis

ZnTCPP titanate nanotubes were synthesized by a hydrothermal process. In this process, 2.6g ZnTCPP-TiO_2 gel was added into a 10M NaOH aqueous solution. After homogeneous mixing, the specimen was transferred into a sealed Teflon container statically heated at 140□ for 24h. Then the product was washed with 0.1M hydrochloric acid until the pH value of the product dropped to 7. Dry for 12 h at 100□. Finally, the above product were calcined at different temperature in the muffle furnace, for example calcining to 100□、200□、300□and 400□ for 4h, then we obtained our target materials.

2.4 Adsorption of MB on ZnTCPP-TNTS

The sorption experiments were carried out in glass container at room temperature in complete darkness. 50mg ZnTCPP-TNTS sample was added into 100 mL of aqueous dye solution at the concentration of 20mg/L. The preliminary experiment revealed that 15 minutes was required for the adsorption process to reach equilibrium. After stirring 15 minutes, the sample solution was centrifuged to remove ZnTCPP-TNTS from solution. The solution obtained this way was extracted into a quartz cell. The absorbance of the samples was measured with quartz cells every 5 min. The adsorption capacity of MB was then calculated using the relation q=V△C/m, where V was the volume of the liquid phase, m mass of the solid, and △C was the difference between the initial and final concentration of MB.

3 Results and discussion

3.1 Morphology

Figure 1 shows the scanning electron microscope (SEM) and transmission electron microscope (TEM) images of the samples prepared at different calcined temperature or sensitizer. The influence of calcined temperature on the morphology of the ZnTCPP-TNTS is noticeable in figures 1(A,B,C,D) and (E,F), depicting the products synthesized at 200, and 400□, respectively. sodium titanate calcined at 200□, no matter what they sensitized, consist of long straight nanotubes with open ended lying on the substrate in various random directions, with an average diameter of 15 nm and the length of several hundreds of nanometers, which is in good agreement with many previous reports[29-31]. The mechanism for the nanotube formation has been explained as the folding of nanosheet under asymmetric surface tension[32]. though a comparison of their images reveals that the ones prepared with no ZnTCPP sensitizer are more aggregated. With the ZnTCPP sensitized on the surface, the nanotubes are well separated (figures 1(C,D)), but still keeps the tubes morphology, which indicated that the presence of ZnTCPP molecules have modified the surface electrostatic properties, though it is still keep enough drive for the wrapping action. The mixture of sodium titanate and anatase TiO_2 grown at 400□, on the other hand, have formed agglomerated nanoparticles and nanorods (figures 1(E,F)).

3.2 Phase composition

The XRD spectra of the as-synthesized ZnTCPP-TNTS at different calcined temperature and P25 are shown in Fig. 2. The samples prepared at lower temperatures (ZnTCPP-TNTS-100 □ and ZnTCPP-TNTS-200 □) exhibits two very broad peaks near 24.4°and 48.4°, which can be assigned

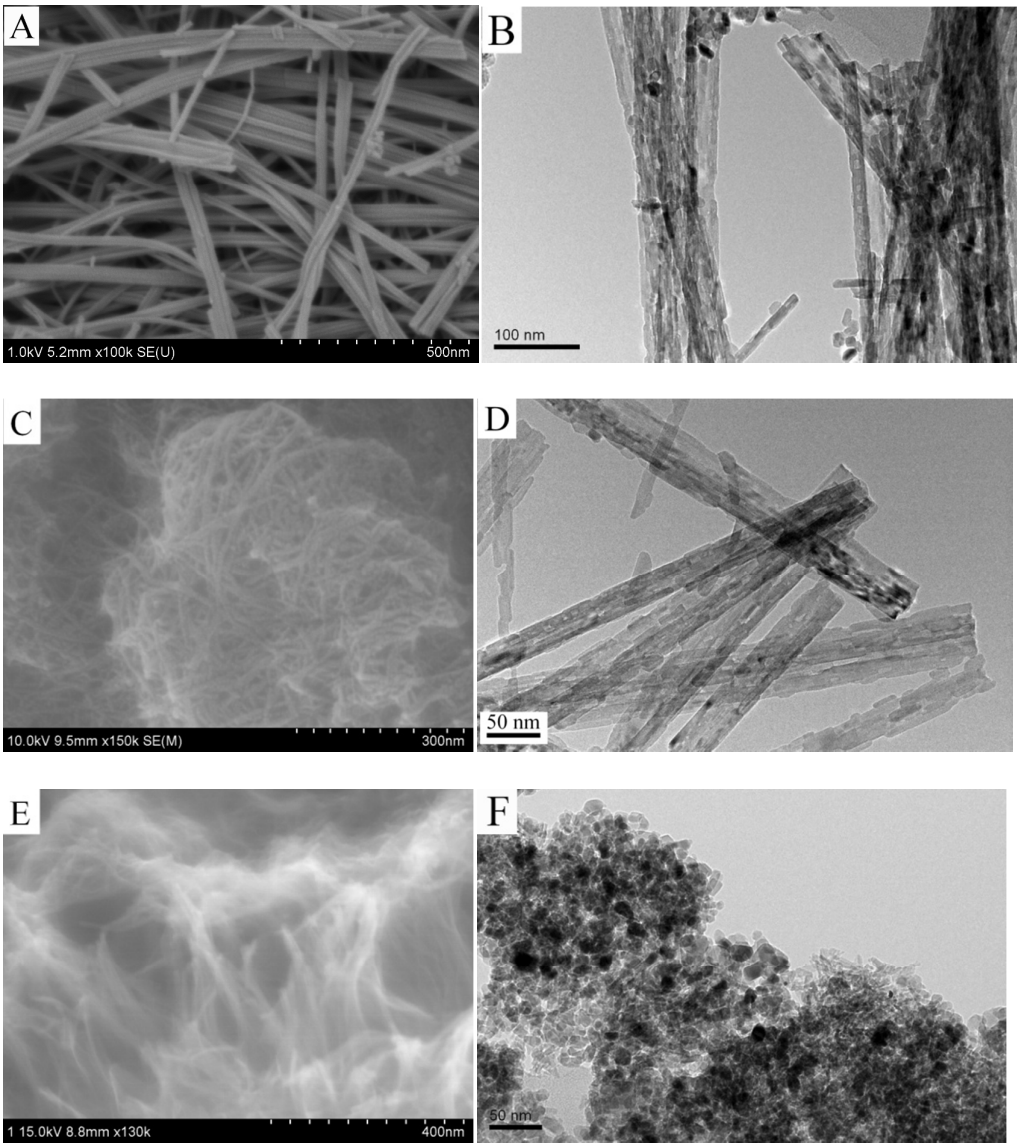

Figure 1. Effect of calcined temperature (C,D at 200℃ and E,F at 400℃) and sensitizer ZnTCPP (A,B are TNTS and C-F are ZnTCPP-TNTS) on the morphology of ZnTCPP-TNTS, as revealed by SEM (A,C,E) and TEM(B,D,F).

to an amorphous or poorly crystallized sodium titanate phase. The broadening of diffraction peaks in the patterns indicates that the crystal size of ZnTCPP-TNTS-100 □ and ZnTCPP-TNTS-200 □ samples is fine (as confirmed by SEM and TEM images). When the nanotubes were calcined at 300□,the Ωpeak at 24.4°and 48.4°exhibited a shoulder peak, indicating a new crystal form appears. these shoulder peak at 25.3°and 48°are in good agreement with the standard XRD patterns of anatase crystal faces (101) and (200) respectively. The intensity of these shoulder peak increase when the calcined temperature rise from 200 ℃ to 400 ℃. This suggests that the TNTS partly transformation to anatase form when the calcined temperature enhanced. For the sample of ZnTCPP-TNTS-300 □sodium titanate still remained as the predominant phase, with a small amount of anatase, as seen from the relative weak intensities of the shoulder peaks. At the

calcination temperature of 400℃, the crystal faces of anatase (101)、anatase (200)、anatase (105) and anatase（211）were obviously present, the peak of which were strong, and these peaks were found to be in good agreement with the standard XRD patterns of anatase. While the peak at 24.4°and 48.4°are also present, indicating there coexists the sodium titanate phase. These can also be confirmed by SEM and TEM images.

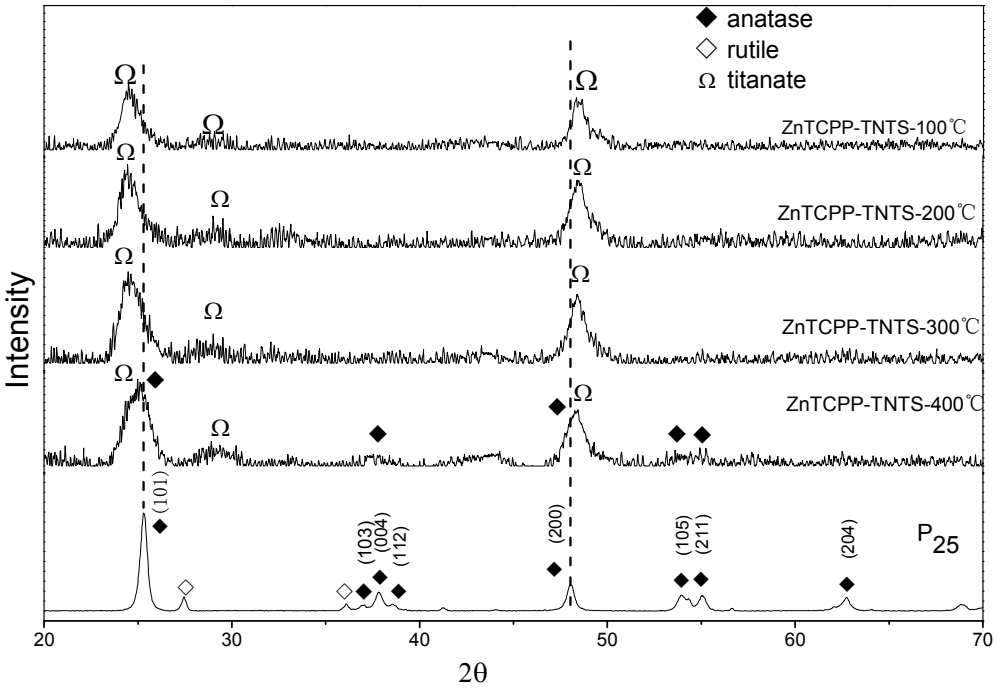

Figure 2 XRD patterns of ZnTCPP-TNTS at different calcined temperature, and P25 were show for comparison. ◆stands for anatase, ◇for rutile and Ω for titanate.

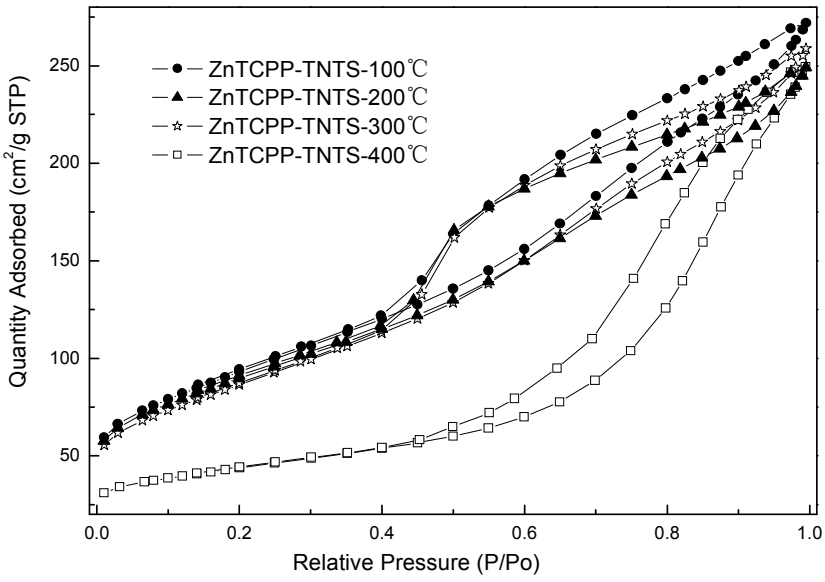

Figure 3 Adsorption/desorption isotherms of N_2 onto ZnTCPP-TNTS

Table 1 Surface characteristics of ZnTCPP-TNTS determined from N_2 physisorption

Sample	Surface Area (m^2/g)	Pore Size (nm)	Pore Volume (cm^3/g)
ZnTCPP-TNTS-100℃	335.3083	4.80002	0.402372
ZnTCPP-TNTS-200℃	322.1042	4.54253	0.365792
ZnTCPP-TNTS-300℃	311.4199	4.88566	0.380373
ZnTCPP-TNTS-400℃	154.1421	9.44472	0.363957

.

3.3 N_2 adsorption–desorption isotherms

The nitrogen adsorption–desorption isotherms were carried out to characterize the surface layer of the as-synthesized samples fabricated with different calcination temperature. According to the isotherms shown in Figure 3 all the ZnTCPP-TNTS isotherms could be identified as the type IV (IUPAC classification), which were characteristic of mesoporous materials[33]. In addition, the hysteresis loop of ZnTCPP-TNTS-100℃, ZnTCPP-TNTS-200℃ and ZnTCPP-TNTS-300℃resemble H4 in the IUPAC classification, while the hysteresis loop of ZnTCPP-TNTS-400℃resemble H3, indicating that the former three lower temperature samples comprised of aggregates of platy wrapped tubes containing open slit-shaped pores with fairly wide bodies and narrow short narrow necks, while the ZnTCPP-TNTS-400℃samples associated with nanoparticles and nanorods (loose assemblages) exhibiting a narrow distribution of relatively uniform slit-like pores, this characterization is consistent with the result from TEM and XRD measurements, the higher temperature collapsed the nanotubes and transformations the crystal form from the sodium titanate phase to anatase. In addition, the former three lower temperature samples display a relatively stronger adsorption of N2 molecules in the low-pressure (p/p0) region than ZnTCPP-TNTS-400℃ do, implying that ZnTCPP-TNTS-400℃ make little contribution to the nitrogen adsorption while the other three lower temperature samples owns excellent adsorption ability. Accordingly, as listed in Table 1, The Brunauer-Emmett-Teller (BET) specific surface area of ZnTCPP-TNTS calcined at lower temperature is more than twice that of ZnTCPP-TNTS-400℃, indicating the effectiveness of calcined temperature and the corresponding crystal form in decreasing the surface area. The pore volumes and pore size for the as-synthesized samples are also included in Table 1.

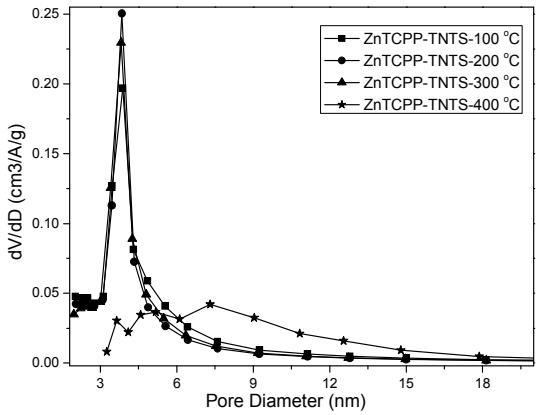

Figure 4 pore size distributions of ZnTCPP-TNTS from adsorption

The pore-size distribution was analyzed from desorption branch data analysis based on the Barrett–Joyner–Halenda (BJH) method, and the results are shown in Fig. 4. Fig 4 shows that the pore-size distribution are nearly unchanged when the calcined temperature raised from 100℃ to 300℃, they characterized with a narrow intense signal and a pore size maximum at a radius of 3.8 nm. the pore-size distribution of ZnTCPP-TNTS-400℃, however, possesses prominent different patterns with a broad range of pore diameter from 3.8 nm to 18 nm. The pore diameter of 3.8 nm is attributed to the inner diameter of sodium titanate TNTs, while the broad range of pore diameter is ascribed to the interaggregation of sodium titanate TNTs on the surface of anatase TiO_2 particles.

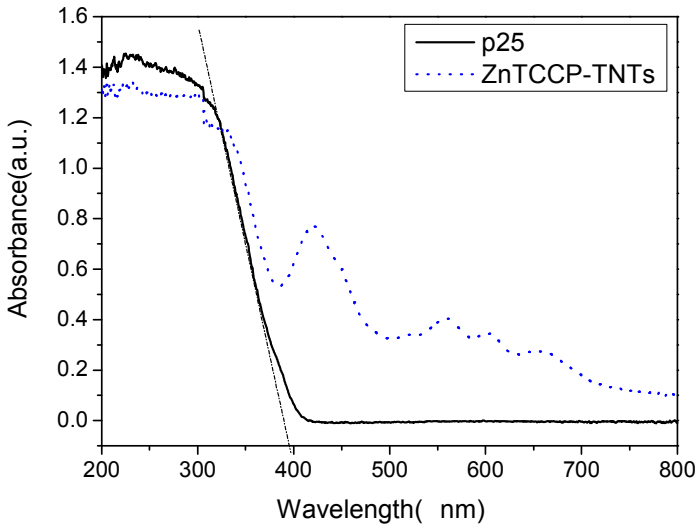

Figure 5 the UV-vis diffuse reflectance spectra of P25 and ZnTCPP-TNTS-100℃

Fig. 5 shows the UV-vis diffuse reflectance spectra (DRS) of P25 and the as-prepared ZnTCPP-TNTS-100℃. Clearly, the largest absorption edge of pure P25 was at approximately 390nm, which are in good agreement with the reported values of P25 (Eg =3.2 eV, corresponding to λ=387 nm). Due to the strong absorption of ZnTCPP in Soret band at 429nm and Q band at 560~670nm, ZnTCPP-TNTS-100℃ displayed enhanced multi-peak absorption in the visible-light region, the absorption is even extended to lager than 800nm. The optical absorption onsets of ZnTCPP-TNTS-100℃ shifted to the lower energy region. This suggested that the ZnTCPP-TNTS-100℃ particles could absorb light over a quite broad spectral range in the visible region, which is a prerequisite for the utilization of visible light for photocatalysis. Therefore, good photochemical and photocatalytic activities of ZnTCPP-TNTS-100℃ under visible light irradiation are expected.

3.4 Time resolved spectroscopy characterization

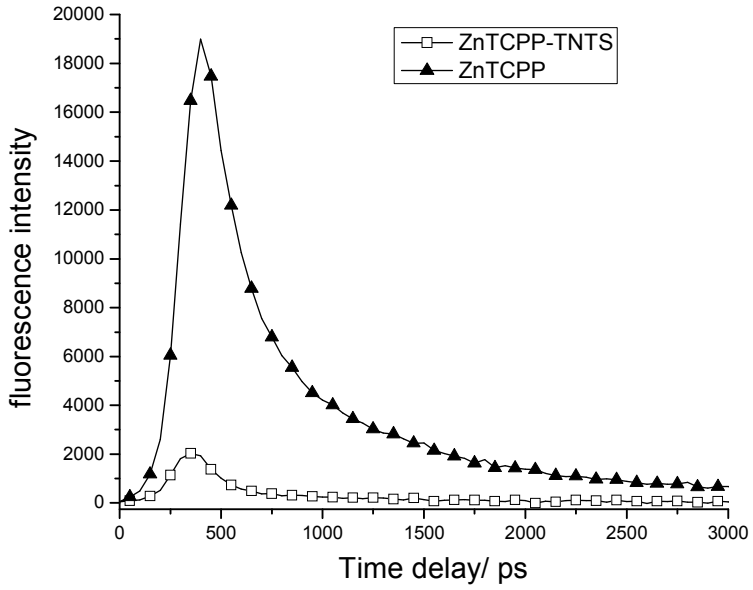

Figure 6 Fluorescence decay profiles of ZnTCPP and ZnTCPP-TNTS-100℃ obtained by TCSPC.

Fig. 6 shows the fluorescence decay profiles of ZnTCPP and ZnTCPP coupled titanate nanotubes (ZnTCPP-TNTS-100℃) respectively. It shows that in our experiment, the fluorescence of ZnTCPP is quenched by titanate nanotubes after UV excitation(370nm), and its lifetime becomes shorter as shown in Fig. 6. This means that under UV excitation electrons transferred from ZnTCPP excited state to the nanotubes conduction band and consequently quenched the emission intensity of ZnTCPP fluorescence process. On other hand it also verifies that the ZnTCPP is chemically linked to the bulk of titanate nanotubes. This observation is in consistency with the literature reported[34]

It is well known that the recombination of photo-generated electrons and holes In nano-sized TiO_2 occurs in several microseconds under vacuum conditions[25]. We also characterized the ZnTCPP- TNTS-100℃with Transient absorption spectroscopy in the femtoseconds to study the recombination processes of electrons and holes.

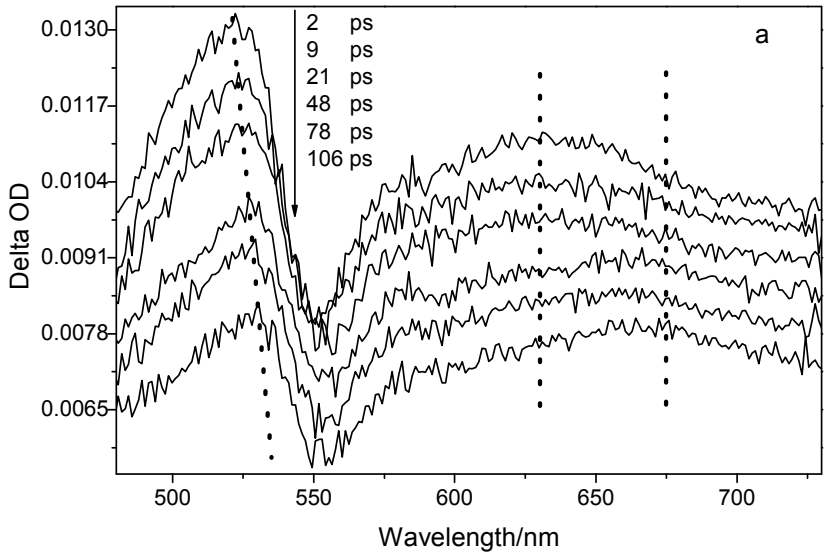

Figure 7 Femtosecond Transient absorption spectra of ZnTCPP-TNTS-100℃ in MeCN in the spectral range 430-730 nm exciting at 400 nm with femtosecond pulses. The transient spectra are plotted in sequence (from up to low) with the increase of the delay time between pump and probe pulse.

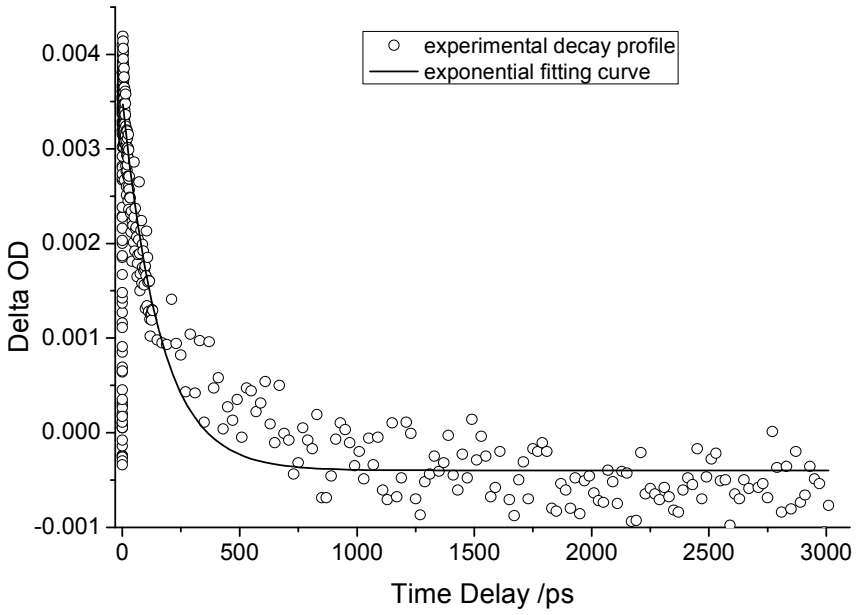

Figure 8 Transient absorption decay profile of ZnTCPP- TNTS-100℃ in MeCN exponential function fitting curve is shown as black line and the experimental decay profile shown as circles.

Fig. 7 presents the Femtosecond TA spectra of ZnTCPP- TNTS-100℃ dispersed in MeCN. We used MeCN as the solvent to disperse the ZnTCPP- TNTS-100℃ because Acetonitrile (MeCN) is a slow hole scavenger of TiO_2 and the reaction between MeCN and holes is not detected on the

femtosecond time scale. As shown in Fig. 7, there are three absorption bands which site at 530nm, 630 nm and 680nm respectively, the 530nm and 630nm absorption band is assigned as trapped holes absorption on TiO_2 and the 680nm absorption band lies in an overlap region of the trapped holes absorption band and the trapped electrons absorption band[35]. a precise assignment of the absorptions of electrons and holes is rather difficult because their absorption spectra are very broad and the bands overlap each other, moreover, the TiO_2 transient absorption is sensitive to the particle size, crystal phase, and surface conditions. In Fig. 7, the appearance of trapped holes at 530nm (or 630nm) and the trapped electrons at 680nm suggest that some holes and electrons are photogenerated and are trapped separately; The peak at 530 nm and 630nm generate and decay in the same step. The 530nm absorption showed a slight red-shift with the increase of the delay time, probably due to the decay of the shallower trapped holes. Fig.8 shows the 637nm TA decay profiles of ZnTCPP- TNTS-100℃. We observed that the recombination of photo-generated electrons and holes in the ZnTCPP TNTS-100℃ took place in about 159 picoseconds, which is 3000 times faster than in nano-sized TiO_2 as shown in ref [36]. The shorter lifetime of holes onto the sensitizer modified TiO_2 surface could give rise to a decrease of oxidation reactions with adsorbed species, this could explains why the visible light activity of dye sensitized TiO_2 is still largely lag behind the UV light activity of TiO_2.

3.5 Adsorptive properties of ZnTCPP-TNTS

As mentioned above, the as-synthesized TNTS Exhibit 3D surface layer and a large specific surface area, thus, their adsorptive properties were firstly evaluated by using Methylene Blue (MB) solution as the target pollutant. The adsorption tests were carried out in the dark to prevent the degradation of MB under light. Fig. 9 shows the temperature dependent of adsorption quantity of MB with time on the ZnTCPP-TNTS calcined in the muffle furnace with different temperature. It is clear that the adsorption process quickly reach to equilibrium in 60 min, the final equilibrium adsorption quantity of the as-synthesized ZnTCPP-TNTS samples make no obvious difference in the 20mg/L MB solution. With the increasing of calcined temperature,

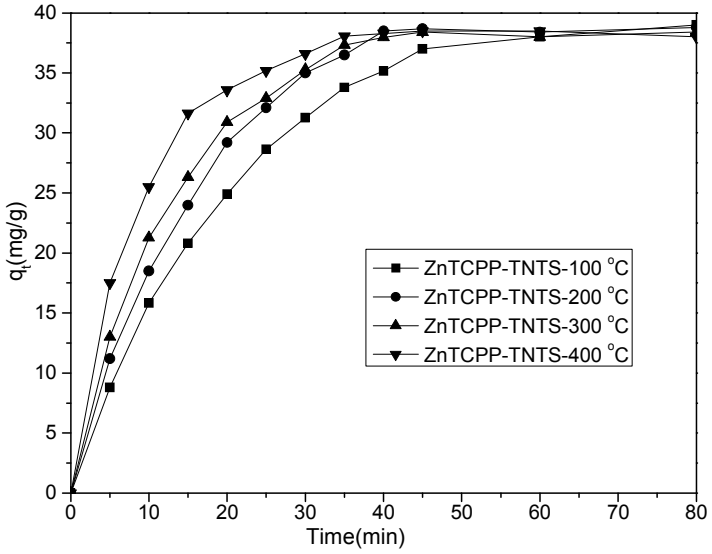

Fig 9. Effect of calcined temperature on the adsorption quantity of MB with 50mg of ZnTCPP-TNTS in the MB solution (20mg/L) at room temperature and pH 6

the loss in the specific surface area(Table 1) was compensated by an increase in the number of surface active sites for the adsorption of methylene blue, however the time reaches to the adsorption equilibrium becomes shorter. This could be easily explained by the structure that measured by N_2 adsorption-desorption hysteresis loop, lower temperature calcinated nanotube with wide bodies and narrow necks made the large specific surface area unreachable for relatively big MB molecule, then prolong the equilibrium absorption time, and some surface area is wasted. But for higher temperature calcinated broken tube with uniform slit-like pores made the every surface area exposure outside and attainable for all MB, thus accelerates the equilibrium time and the all active surface area are utilized.

The adsorption kinetic of MB on the ZnTCPP-TNTS was also investigated(Figure 10). Their adsorption kinetic curves can be described well by the pseudo second-order rate model with high correlation coefficients (R > 0.99) as follows: $\frac{t}{q_t} = \frac{1}{kq_e^2} + \frac{t}{q_e}$ where qe is the equilibrium adsorption capacity, qt is the adsorption capacity at t, t is the reaction time, and k is the pseudo-second-rate constant. The slope increases as the calcined temperature goes up. Similar kinetics model has also been observed in the adsorption of MB onto titanate nanostructures[37]

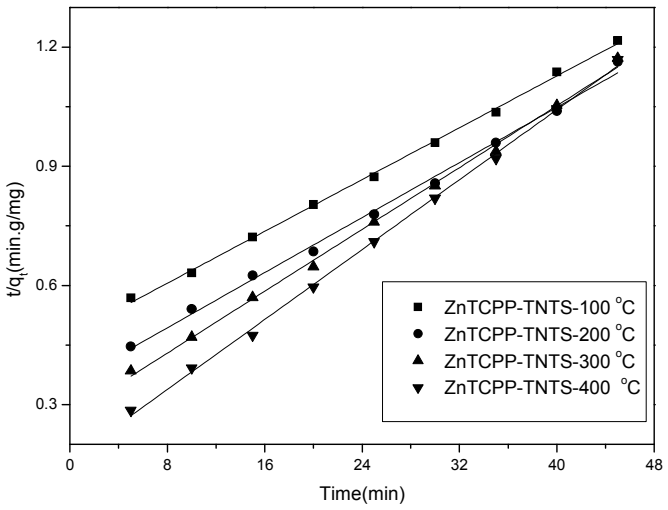

Figure 10 The adsorption kinetic curves of MB on the ZnTCPP-TNTS calcined in the Muffle at different Temperature (20 mg/L, pH = 6).

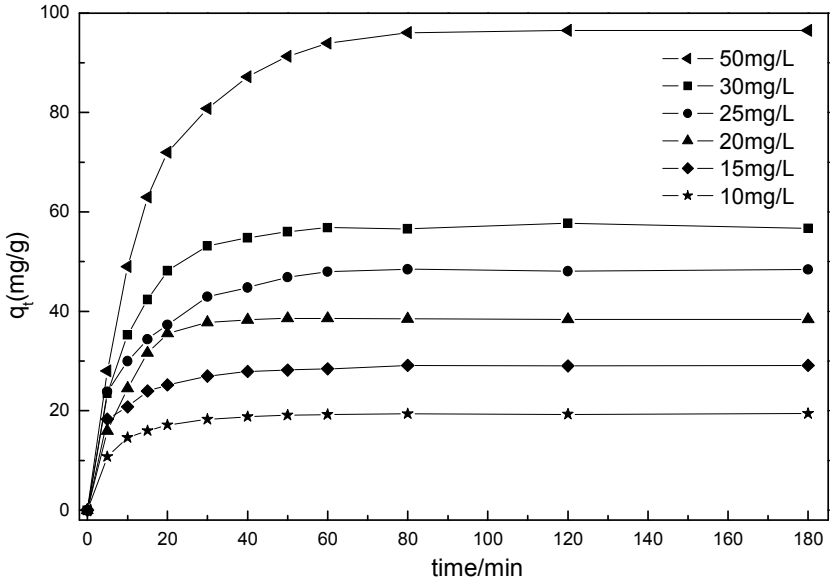

Figure 11. The time dependent of adsorption quantity on the ZnTCPP-TNTS-300℃ in MB solutions with different concentrations.

3.6 Adsorption isotherm

To investigate the MB adsorption capacities of the as-synthesized ZnTCPP-TNTS, adsorption isotherm tests were carried out. Adsorption isotherm describes adsorption mechanism between absorbent and adsorption by the comparison with the theoretical analysis and the experimental data. The main types of Adsorption isotherm are Langmuir adsorption isotherm and Freundlich adsorption isotherm. The Langmuir adsorption isotherm:

$$\frac{1}{q_e}=\frac{1}{q_{\mathrm{m}}}+\frac{1}{q_{\mathrm{m}}K_L}\frac{1}{C_e} \quad (1)$$

Where q_m is the maximum adsorption capacity,and K_L is the Langmuir constant. If the adsorption isotherm exhibits Langmuir behavior, it indicates monolayer adsorption.

And the Freundlich adsorption isotherm:

$$\log q_e = \log K_f + \frac{1}{n}\log C_e \quad (2)$$

Where K_f and n are the Freundlich constants indicating the adsorption capacity and adsorption intensity, respectively. a good fit into the Freundlich model indicates a heterogeneous surface binding.

In this experiment The sample ZnTCPP-TNTS-300℃ was chosen to perform the adsorption experiments. Fig. 11 shows the effects of MB concentrations on the equilibrium absorption quantity. To understand the adsorption mechanism, the equilibrium adsorption isotherm data were curve-fitted into the Freundlich and Langmuir models and the results were summarized in Table 2.

Table 2 Langmuir and Freundlich isotherm constants for the adsorption of MB onto ZnTCPP-TNTS-300℃.

Langmuir				Freundlich		
q_e^a	K_L^b	q_m^c	R^2	K_f^d	n	R^2
96.50	0.48	158.23	0.95	51.11	1.32	0.88

Our experiment shows that the Regression coefficients of Langmuir adsorption isotherm is 0.95,which is higher than that of Freundlich adsorption isotherm(R^2=0.88).So zinc carboxyl porphyrin nanotubes at 300℃ mostly conforms to Langmuir adsorption model of single molecule layer absorption. Compared with existing data in the literature[38], the ZnTCPP sensitized titanate nanotubes synthesized in this work qm1 (158.23 mg/g) exhibited relative higher adsorption capacities. The adsorption mechanism may be due to an electrostatic force of attraction between the adsorbent and MB. the enhanced adsorption capacities could be explained that although the sensitizer occupied some adsorption sites, abundant carboxyl groups in alkaline enhanced the negative surface charge for titanate, MB, a cationic dye, can be attracted by titanate nanostructures via an electrostatic force of attraction.

3.7 Adsorption recycling experiment

The hierarchical ZnTCPP sensitized TiO_2 nanotubes can be easily recycled by a simple centrifugation and calcination. After five recycles for the adsorption of MB, the ZnTCPP-TNTS calcined at 300 °C still showed good activity (Figure 12). Our study indicates that the sorbent possesses excellent stability and reusability, which is important for practical applications such as environmental depollution.

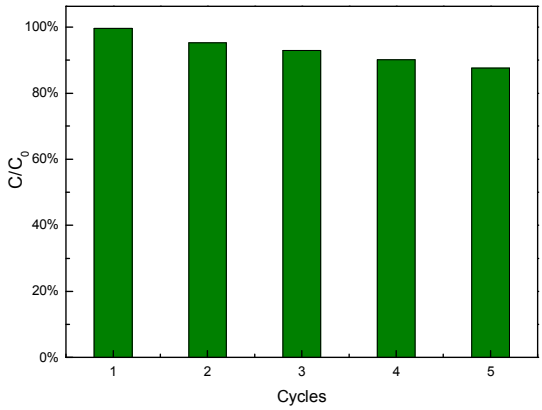

Figure 12. Cyclic runs of the absorption of MB (20 mg/L) in the presence of the ZnTCPP-TNTS-300℃. The running time is 60 min for every cycle. pH=6

3.8 Photocatalytic Activity of ZnTCPP-TNTS.

It is well known that the photocatalysis activity depends on the crystallinity, phase, and the surface area of the materials. In this work, the visible light induced photocatalytic activities of the as-synthesized ZnTCPP sensitized TiO_2 nanotubes were evaluated by photocatalytic degradation of MB under 250 W Iodine-Tungsten lamp illumination with 420 nm cutoff filter. Experiments in the dark and under visible light were performed to distinguish the contribution of adsorption and

degradation[24]. The Degussa P25 titania nanoparticles (P25, surface area ~40 m^2/g with a particle size of ~21 nm) was selected for comparison. As shown in Figure 13, P25 show little degradation of MB in visible light irradiation due to its poor surface area and large band-gap. The other calcined samples can efficiently absorption and photodegrade MB under visible light irradiation. in the MB adsorption and photodegradation process as observed in Figure 13, over 99.9% （$(1-C/C_0)\times100\%$in 45min)of the dye in bulk solution removed under visible light irradiation, blank experiment with dark adsorption contributed to the reduction of 94% in MB concentration, indicating the significant adsorption capacity of the ZnTCPP-TNTS in the whole process. The high efficiency performance could be ascribed to its unique cooperative effects of large surface area, strong adsorption ability and low band gap energy. Larger specific surface area implies that the number of hydroxyl group and carboxyl is higher; more active sites can be obtained and allows more aqueous reactants, water or O_2 to be absorbed onto the surface of the photocatalyst, The adsorbed molecular O_2 can efficiently capture photogenerated electrons to form active O_2^- species and therefore leads to higher photocatalytic activity while higher pore volume results in a more rapid diffusion of various aqueous products during the photocatalytic reaction and reduce the volume charge–carrier recombination and ensure the escape of e−/h+ pairs to the surface. ZnTCPP sensitizer with smaller band gap means that the adsorbents can absorb light with higher wavelengths and therefore are more photoefficient.

The visible light photodegradation can promote the removal of MB during the adsorption system and maybe it could be used to regenerate the ZnTCPP-TNTS absorbers.

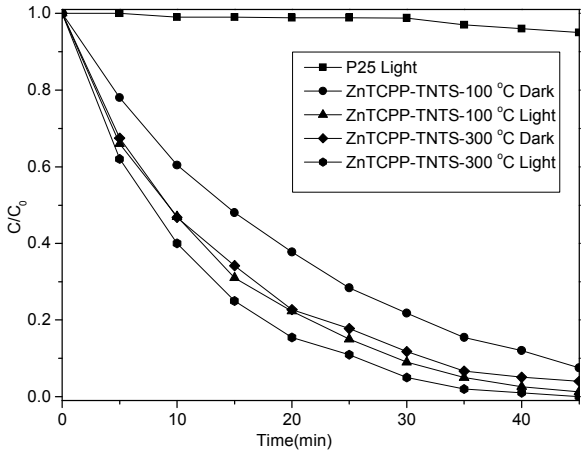

Figure 13 Evolution of MB concentration as a function of time

4 Conclusions

ZnTCPP-TNTS were prepared by Sol-Gel Method using tetrabutyl titanate and ZnTCPP as precursors, followed by hydrothermal treatment of ZnTCPP-TiO_2 gel and then calcined for 2 h.

The following changes were observed in the physicochemical properties of the **ZnTCPP-TNTS** when calcination treatment of TNTS from 100°C to 400°C: the crystalline phase are partly transformation from sodium titanate to anatase, a decrease in the specific surface area, the morphology change from nanotubes to nanoparticles and nanorods. Calcination also caused an

increase in the number of hydroxyl group and carboxyl active sites for the MB adsorption.

The properties of photo-generated holes and electrons were studied by transient absorption spectroscopies.

The presence of ZnTCPP-molecules in the TiO_2 nanotube surface led to a significant enhancement in its MB adsorption capacity. The equilibrium data fitted well with the Langmuir model, and the kinetics of dye adsorption followed the pseudo-second-order model. The ZnTCPP-TNTS could easily be reclaimed and shows excellent stability and reusability.

The development of the porphyrin-based photocatalyst provides an alternative approach in harnessing solar visible light. Further investigations about the adsorption and photocatalysis behaviors should be made to obtain deeper insight into the cooperative action mechanism between them.

Acknowledgements

This work was supported by grants from Alexander von Humboldt Foundation, National Natural Science Foundation of China (No. 21271155 and 21473161), Natural Science Foundation of Zhejiang Province (No. LY13B030009) and Zhejiang SCI-TECH University for 521 Distinguished Scholars scheme.

References

1 M. B. Zakaria, N. Suzuki, K. Shimasaki, N. Miyamoto, Y. T. Huang and Y. Yamauchi, *Journal of Nanoscience and Nanotechnology*, 2012, **12**, 4502-4507.

2 T. Nonoyama, T. Kinoshita, M. Higuchi, K. Nagata, M. Tanaka, K. Sato and K. Kato, *Journal of the American Chemical Society*, 2012, **134**, 8841-8847.

3 J. H. Shen, Y. H. Zhu, X. L. Yang and C. Z. Li, *Journal of Materials Chemistry*, 2012, **22**, 13341-13347.

4 S. Liu, E. Y. Guo and L. W. Yin, *Journal of Materials Chemistry*, 2012, **22**, 5031-5041.

5 T. Ohno, K. Sarukawa, K. Tokieda and M. Matsumura, *Journal of Catalysis*, 2001, **203**, 82-86.

6 L. L. Dou, L. S. Gao, X. H. Yang and X. Q. Song, *Journal of Hazardous Materials*, 2012, **203**, 363-369.

7 J. Ananpattarachai, P. Kajitvichyanukul and S. Seraphin, *Journal of Hazardous Materials*, 2009, **168**, 253-261.

8 R. Asahi, T. Morikawa, T. Ohwaki, K. Aoki and Y. Taga, *Science*, 2001, **293**, 269-271.

9 A. Di Paola, E. Garcia-Lopez, G. Marci and L. Palmisano, *Journal of Hazardous Materials*, 2012, **211**, 3-29.

10 H. M. Ding, H. Sun and Y. K. Shan, *Journal of Photochemistry and Photobiology a-Chemistry*, 2005, **169**, 101-107.

11 S. G. Kumar and L. G. Devi, *Journal of Physical Chemistry A*, 2011, **115**, 13211-13241.

12 M. Pelaez, N. T. Nolan, S. C. Pillai, M. K. Seery, P. Falaras, A. G. Kontos, P. S. M. Dunlop, J. W. J. Hamilton, J. A. Byrne, K. O'Shea, M. H. Entezari and D. D. Dionysiou, *Applied Catalysis B-Environmental*, 2012, **125**, 331-349.

13 M. K. Panda, K. Ladomenou and A. G. Coutsolelos, *Coordination Chemistry Reviews*, 2012, **256**, 2601-2627.

14 C. Wang, J. Li, G. Mele, G. M. Yang, F. X. Zhang, L. Palmisano and G. Vasapollo, *Applied Catalysis B-Environmental*, 2007, **76**, 218-226.

15 F. Odobel, E. Blart, M. Lagree, M. Villieras, H. Boujtita, N. El Murr, S. Caramori and C. A. Bignozzi, *Journal of Materials Chemistry*, 2003, **13**, 502-510.

16 J. Y. Jing, M. H. Liu, V. L. Colvin, W. Y. Li and W. W. Yu, *Journal of Molecular Catalysis a-Chemical*, 2011, **351**, 17-28.

17 J. Q. Huang, Y. G. Cao, Z. H. Deng and H. Tong, *Journal of Solid State Chemistry*, 2011, **184**, 712-719.

18 T. Wang, W. Liu, N. Xu and J. R. Ni, *Journal of Hazardous Materials*, 2013, **250**, 379-386.

19 A. K. L. Sajjad, S. Shamaila and J. L. Zhang, *Journal of Hazardous Materials*, 2012, **235**, 307-315.

20 Y. X. Tang, D. G. Gong, Y. K. Lai, Y. Q. Shen, Y. Y. Zhang, Y. Z. Huang, J. Tao, C. J. Lin, Z. L. Dong and Z. Chen, *Journal of Materials Chemistry*, 2010, **20**, 10169-10178.

21 Y. X. Tang, Y. K. Lai, D. G. Gong, K. H. Goh, T. T. Lim, Z. L. Dong and Z. Chen, *Chemistry-a European Journal*, 2010, **16**, 7704-7708.

22 S. Qourzal, M. Tamimi, A. Assabbane and Y. Alt-Ichou, *Journal of Colloid and Interface Science*, 2005, **286**, 621-626.

23 D. Robert, S. Parra, C. Pulgarin, A. Krzton and J. V. Weber, *Applied Surface Science*, 2000, **167**, 51-58.

24 Y. X. Tang, Z. L. Jiang, Q. L. Tay, J. Y. Deng, Y. K. Lai, D. G. Gong, Z. L. Dong and Z. Chen, *Rsc Advances*, 2012, **2**, 9406-9414.

25 Y. Y. Zhang, Y. X. Tang, X. F. Liu, Z. L. Dong, H. H. Hng, Z. Chen, T. C. Sum and X. D. Chen, *Small*, 2013, **9**, 996-1002.

26 M. Grandcolas, A. Louvet, N. Keller and V. Keller, *Angewandte Chemie-International Edition*, 2009, **48**, 161-164.

27 Y. M. Xu and C. H. Langford, *Langmuir*, 2001, **17**, 897-902.

28 W. Kim, J. Park, H. J. Jo, H. J. Kim and W. Choi, *Journal of Physical Chemistry C*, 2008, **112**, 491-499.

29 P. M. Rorvik, T. Grande and M. A. Einarsrud, *Advanced Materials*, 2011, **23**, 4007-4034.

30 D. V. Bavykin, V. N. Parmon, A. A. Lapkin and F. C. Walsh, *Journal of Materials Chemistry*, 2004, **14**, 3370-3377.

31 Y. B. Mao, S. Banerjee and S. S. Wong, *Journal of the American Chemical Society*, 2003, **125**, 15718-15719.

32 A. Kukovecz, M. Hodos, Z. Konya and I. Kiricsi, *Chemical Physics Letters*, 2005, **411**, 445-449.

33 M. Thommes, *Chemie Ingenieur Technik*, 2010, **82**, 1059-1073.

34 A. Kathiravan, P. S. Kumar, R. Renganathan and S. Anandan, *Colloids and Surfaces a-Physicochemical and Engineering Aspects*, 2009, **333**, 175-181.

35 T. Yoshihara, R. Katoh, A. Furube, Y. Tamaki, M. Murai, K. Hara, S. Murata, H. Arakawa and M. Tachiya, *Journal of Physical Chemistry B*, 2004, **108**, 3817-3823.

36 L. H. Yu, J. Y. Xi, M. D. Li, H. T. Chan, T. Su, D. L. Phillips and W. K. Chan, *Physical Chemistry*

Chemical Physics, 2012, **14**, 3589-3595.

37 J. Q. Huang, Y. G. Cao, Z. G. Liu, Z. H. Deng and W. C. Wang, *Chemical Engineering Journal*, 2012, **191**, 38-44.

38 Y. W. L. Lim, Y. X. Tang, Y. H. Cheng and Z. Chen, *Nanoscale*, 2010, **2**, 2751-2757.

Effect of calcined temperature and sensitizer ZnTCPP on the morphology of ZnTCPP-TNTS.

Huigang Wang, Ying Fu, Dongmei Zhou, Junmin Wan and Xuming Zheng